Original Article | Thoracic Imaging

https://doi.org/10.3348/kjr.2018.19.5.872
pISSN 1229-6929 · eISSN 2005-8330
Korean J Radiol 2018;19(5):872-879

Korean Journal of Radiology
KJR

Cone-Beam CT Virtual Navigation-Guided Percutaneous Needle Biopsy of Suspicious Pleural Metastasis: A Pilot Study

Hyun-ju Lim, MD, Chang Min Park, MD, Soon Ho Yoon, MD, Jae Seok Bae, MD, Jin Mo Goo, MD

All authors: Department of Radiology, Seoul National University Hospital, Seoul 03080, Korea

Objective: To evaluate the diagnostic performance of cone-beam computed tomography (CBCT) virtual navigation-guided percutaneous pleural biopsy for suspected malignant pleural disease.

Materials and Methods: This study enrolled 59 patients (31 males and 28 females; mean age, 63.4 years) with suspected malignant pleural disease diagnosed with CBCT from December 2010 to December 2016. Sixty-three CBCT-guided biopsies were performed using a coaxial system with 18- or 20-gauge cutting needles. Procedural details, diagnostic performance, radiation exposure, and complication rates were investigated.

Results: The mean diameter perpendicular to the pleura of 51 focal and 12 diffuse pleural lesions was 1.53 ± 0.76 cm. The mean distance from the skin to the target was 3.40 ± 1.51 cm. Mean numbers of CT acquisitions and biopsies were 3.21 ± 0.57 and 3.05 ± 1.54. Total procedure time and coaxial introducer indwelling time were 11.87 ± 5.59 min and 8.78 ± 4.95 min, respectively. The mean dose area product was 12013.61 ± 7969.59 $mGym^2$. There were 48 malignant, 10 benign, and 5 indeterminate lesions. Sensitivity, specificity, and diagnostic accuracy were 93.8% (45/48), 100% (10/10), and 94.8% (55/58), respectively. Positive and negative predictive values for malignancy were 100% (45/45) and 76.9% (10/13), respectively. Four patients (6.8%) with benign pathology during initial biopsy but still showing a high suspicion of malignancy underwent repeat biopsy and three of them were finally diagnosed with malignant pleural disease. There were three cases of minimal pneumothorax and no grave procedure-related complications.

Conclusion: Cone-beam computed tomography-guided biopsy is an accurate and safe diagnostic technique for suspected malignant pleural lesion with reasonable radiation exposure and procedure time.

Keywords: *Cone-beam computed tomography; Virtual navigation guidance; Pleura; Biopsy; Metastasis*

INTRODUCTION

Diffuse or nodular pleural thickening is a common radiological manifestation in both benign and malignant diseases. However, among pleural lesions presenting with diffuse or nodular pleural thickenings, malignancies, particularly metastases, are more common than benign diseases (1), with approximately 40% of pleural metastases arising from primary bronchogenic carcinoma, 20% from breast carcinoma, 10% from lymphoma and the remaining

Received November 10, 2017; accepted after revision February 6, 2018.
This study was supported by a grant of the Korea Health Technology R&D Project through the Korea Health Industry Development Institute (KHIDI), funded by the Ministry of Health & Welfare, Republic of Korea (grant number: HC15C3390) and a grant of the Industrial Strategic technology development program, funded by the Ministry of Trade Industry and Energy (MI), Republic of Korea (grant number: 10041618).

Corresponding author: Chang Min Park, MD, Department of Radiology and Institute of Radiation Medicine, Seoul National University College of Medicine, 101 Daehak-ro, Jongno-gu, Seoul 03080, Korea.
• Tel: (822) 2072-0367 • Fax: (822) 743-6385 • E-mail: cmpark.morphius@gmail.com

Korean Journal of Radiology
KJR

30% from other primary sites (2). In addition, the diagnosis of pleural metastasis prevents unnecessary surgical interventions in oncological patients (3), and therefore, accurate diagnosis of pleural metastasis is of great clinical importance. Until now, circumferential pleural thickening, pleural nodularity, parietal pleural thickening greater than 1 cm, and mediastinal pleural involvement have been identified specifically in malignant pleural diseases including metastasis (4), although with low sensitivity (5).

The diagnostic accuracy of cytological testing for suspicious malignant pleural effusions ranged between 50% and 60% (6). Thus, pathological diagnosis with solid tissue samples still remains critical, particularly for cytology-negative cases. In this regard, medical thoracoscopy has been routinely performed in many clinics for pleural effusion not diagnosed clinically, radiologically or cytologically as it enables direct visualization of pleural lesions with a diagnostic yield ranging between 91% and 95% for malignant disease with a low rate of major complications. However, it is also known to be invasive, expensive, and currently unavailable in every institution (7, 8). Conversely, image-guided biopsy has several advantages compared with thoracoscopy including the ability to perform biopsy in cases with and without pleural effusion under real-time guidance, with minimal invasiveness, without general anesthesia, at a lower cost, and shorter procedure time. Therefore, ultrasound- or computed tomography (CT)-guided cutting-needle biopsies have frequently been conducted, yielding a diagnostic sensitivity of 76–90.9% (9-14).

Recently, cone-beam CT (CBCT) was introduced to the field of radiological intervention, which was an advance in terms of diagnostic accuracy, safety and efficacy compared with percutaneous transthoracic needle biopsy of lung nodules (15-20) and mediastinal masses (21). In addition, the CBCT virtual navigation software program provides a virtual needle pathway leading to better targeting of lesions, facilitating easy navigation of the needle into the target after initial determination of the skin entry site and destination target based on pre-procedural CBCT data (17).

Nonetheless, to the best of our knowledge, CBCT virtual navigation has not been investigated for pleural biopsy. Therefore, we sought to assess the utility of CBCT virtual navigation system in percutaneous biopsy of pleural lesions in terms of its diagnostic accuracy and complication rates for clinically and radiologically suspected pleural metastasis.

MATERIALS AND METHODS

Study Population

Fifty-nine patients (31 males and 28 females; mean age, 63.4 ± 11.9 years), who had undergone CBCT virtual navigation-guided pleural biopsy for suspected pleural metastasis at our institute between December 2010–December 2016, were included in this retrospective study. We excluded large and superficial lesions, which were examined by ultrasound-guided biopsy. Our Institutional Review Board (IRB) approved this study (IRB No. 1605-105-763). Informed consent was waived by the IRB.

CBCT Virtual Navigation-Guided Pleural Biopsy: Procedure

All biopsies were performed by a board-certified radiologist supervised by radiology staff. Prior to the procedure, contrast-enhanced chest CT scans were reviewed to determine the optimal biopsy site (Figs. 1A, 2A) and the most appropriate needle route, for example, to avoid pathways traversing engorged intercostal vessels. Biopsies were performed using two different CBCT systems, either the AXIOM Artis dTA/VB30 flat-panel detector with a 2048 x 1538 element (Siemens Healthineers, Erlangen, Germany), the Allura Xper FD20 flat-panel detector with a 2480 x 1920 element (Philips Healthcare, Best, the Netherlands) or the Artis Zee multipurpose system flat-panel detector with a 1920 x 2480 element (Siemens Healthineers).

Pre-procedural CBCT scans were obtained to prepare for biopsy (Figs. 1B, 2C). Before scanning, the operating thoracic radiologists educated patients in person for adequate breathing to match the CBCT imaging and the "bull's eye" view during the procedure. The images were then transferred to the virtual navigation software system (iGuide, Siemens Healthineers; XperGuide, Philips Healthcare) and three-dimensional (3D) CT images were reconstructed using multiplanar reformations in axial (Fig. 2B), coronal and sagittal planes. Subsequently, the operator established the target within the lesion and decided the needle entry point at the skin surface, which provided the safest and the most effective route. Usually, the case-tailored access route was selected in the tangential, oblique or angled trajectory to avoid pneumothorax in shallow lesions. By drawing the virtual segment connecting the entry and target points, the operator determined the expected skin-to-target distance (Figs. 1C, 1D, 2D). The operators considered the penetration depth of the cutting

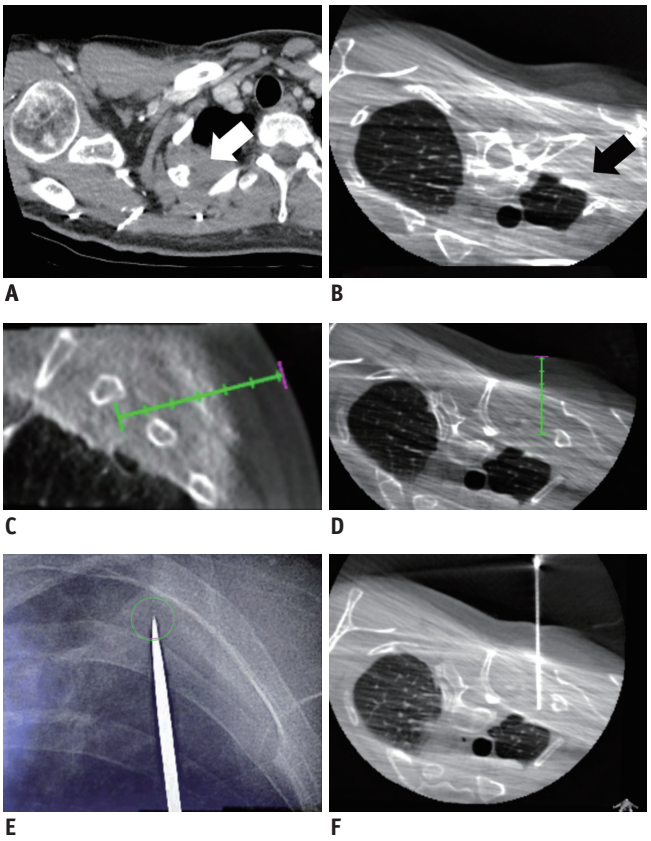

Fig. 1. 44-year-old man diagnosed with AML: example of true positive case of CBCT virtual navigation-guided percutaneous pleural lesion biopsy.
A. Contrast-enhanced diagnostic CT performed prior to procedure showed that possibility of pleural metastasis or AML cannot be excluded for right apical pleural thickening (arrow) in this patient. **B.** Pre-procedural CBCT image shows focal pleural thickening (arrow) in right apical hemithorax. **C, D.** Needle entry site, approach technique and needle advance length are determined in pre-procedural CBCT. **E.** Coaxial introducer needle is introduced into "bull's eye" view of fluoroscopic image, in which skin entry site (pink circle) is superimposed onto target (green circle). **F.** CBCT image shows precise location of tip of coaxial introducer needle within target lesion. Biopsy was performed twice and final pathological diagnosis was involvement of AML. AML = acute myeloid leukemia, CBCT = cone-beam CT

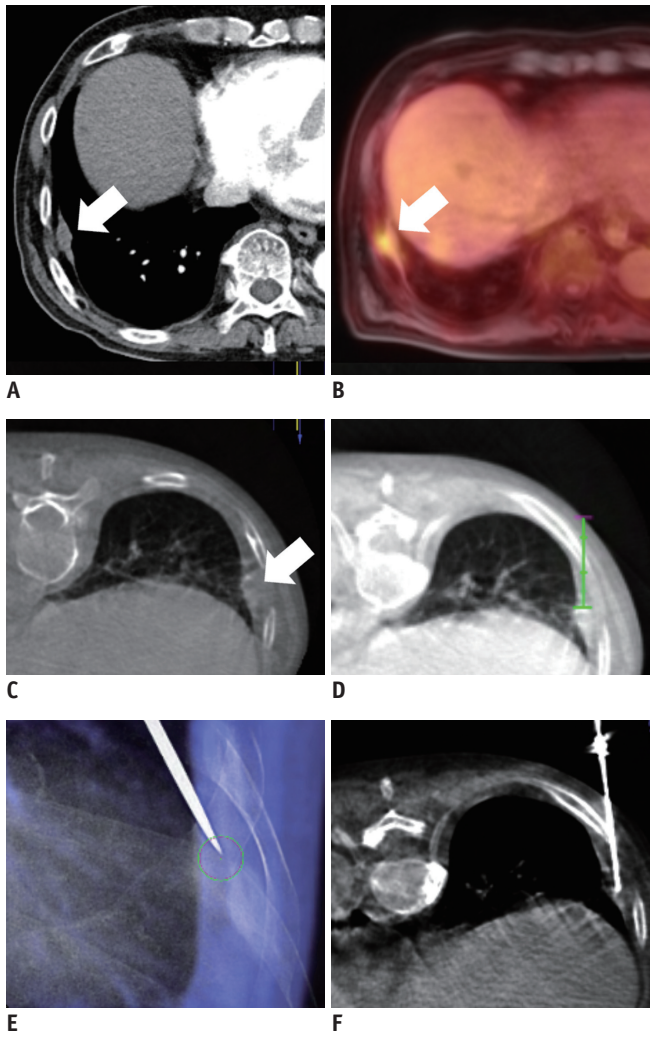

Fig. 2. 81-year-old man with colon cancer and hepatic metastasis: true negative case of CBCT virtual navigation-guided percutaneous pleural lesion biopsy.
A. Pre-procedural contrast-enhanced diagnostic CT shows possibility of pleural metastasis involving right lower pleural thickening (arrow) in this patient. **B.** PET CT performed prior to procedure revealed that this pleural lesion was associated with mild hypermetabolism (arrow). **C.** Pre-procedural CBCT image shows pleural nodular thickening (arrow). **D.** Needle entry site, approach technique and needle advance length are determined in pre-procedural CBCT. **E.** Coaxial introducer needle is introduced into "bull's eye" view of fluoroscopic image, in which skin entry site (pink point) is superimposed onto target (green circle). **F.** CBCT image shows coaxial introducer needle tip within target. Biopsy was repeated twice and final pathological diagnosis suggested chronic granulomatous inflammation with caseous necrosis (acid-fast bacilli-negative, tuberculosis polymerase chain reaction-positive).

needle before firing biopsy gun when they selected the target point. Next, the software automatically calculated the correct C-arm position to display the needle entry point on the patient's skin. According to this data, CBCT moved automatically and the "bull's eye" view (automatic vertical alignment from the skin entry site to the target lesion detected as virtual color spots on the fluoroscopic image) was obtained (Figs. 1E, 2E).

After skin disinfection and local anesthesia (< 10 mL, 1% Lidocaine) at the access area, the operator placed the coaxial introducer needle tip at the cutaneous entry point via fluoroscopy based on the "bull's eye" view. A coaxial introducer was then inserted into the target lesion using the pre-determined skin-to-target distance. Consequently, an intra-procedural CBCT scan was acquired to confirm the appropriate placement of the tip of the coaxial introducer within the target (Figs. 1F, 2F). Biopsy was conducted using either a semi-automatic 18- or 20-gauge cutting

Korean Journal of Radiology
KJR

needle (Stericut, TSK, Tochigi, Japan) until sufficient tissue cores were acquired. The choice of needle size was decided by the operation based on the size of the lesion, intended needle trajectory and operator preference. The number of tissue samples was determined by the operator who macroscopically assessed the biopsy material. Biopsy specimens were formalin-fixed and paraffin-embedded for pathological examination.

Post-procedural CBCT scans were performed to assess any procedural complications after removal of the coaxial introducer needle. After completion of all biopsies, the patient was monitored after absolute bed rest for at least 3 hours. Subsequently, chest radiographs were obtained in the postero-anterior projection with maximum expiration to exclude possible pneumothorax or hemorrhage.

Data Collection

The operators recorded the patient demographics, lesion characteristics (focal or diffuse pleural thickening, lesion size perpendicular to the pleura on diagnostic CT, the distance from the skin to the target on CBCT planning view), procedural details (patients' positions during and after the procedure, the number of biopsies, the number of CT acquisitions, total procedure time (the time from local anesthesia to the end of post-procedural CT), co-axial introducer needle indwelling time and procedure-related complications. Diffuse pleural thickening was defined as thickening of the pleura (more than 5 mm) with an area involving more than 25% of the chest wall if bilateral and 50% involvement if unilateral (22).

We also recorded the dosage of fluoroscopy and CBCT. Total dose-area product (DAP) was measured to determine the absorbed radiation dose (in milligrays, mGy) (16, 17).

Statistical Analysis

We reviewed the pathological reports of biopsy specimens, surgical specimens and follow-up images. We classified the pleural lesions into true-positive, true-negative, false-positive or false-negative results based on the biopsy. The final diagnosis of a pleural lesion was determined according to the following criteria: 1) If the patient underwent surgical resection, the surgical pathology report decided the final diagnosis; 2) If the result of the biopsy revealed a specific malignant or benign pathology such as metastasis or tuberculosis, it was accepted as the final diagnosis. 3) Lesions temporarily labeled as "benign" (e.g., negative for malignancy, chronic inflammation, etc.) and "unresected" were followed up for at least 2 years to ascertain their benign status. Pleural lesions were considered as benign only when the lesions decreased 50% or more in diameter or were stable in size for at least 2 years. 4) If follow-up was less than 2 years, lesions were defined as "indeterminate" and excluded from the statistical analysis.

All data were analyzed using Excel 2010 (Microsoft Corp., Redmond, WA, USA) and SPSS software (version 19.0; IBM Corp., Armonk, NY, USA). Sensitivity, specificity, accuracy, positive predictive value and negative predictive value were recorded. Numeric data were reported as the mean ± standard deviation.

RESULTS

Among 59 patients, 21 were suspected with lung cancer, malignant mesothelioma, or thymoma with pleural metastasis based on imaging results. The remaining 38 patients included 14 diagnosed with lung cancer, 8 cases of breast cancer, 2 cases of thyroid cancer, 2 buccal cancers, 2 patients diagnosed with colon cancer, 3 with hepatocellular carcinoma (HCC), and 1 each of the following patients with cancer: high grade myxofibrosarcoma of the thigh, stomach cancer, tongue cancer, renal cell carcinoma, malignant mesothelioma, lymphoma and acute myeloid leukemia (AML). They underwent a total of 63 pleural biopsies under CBCT guidance. Repeat biopsies for the same lesion were performed in 4 patients with initial benign pathology but with a high suspicion of malignancy, and each was evaluated as an independent case.

Lesion Characteristics, Procedural Records and Radiation Doses

Lesion characteristics and procedural records are summarized in Table 1. Fifty-one cases included focal disease and 12 were diffuse pleural disease in contrast-enhanced diagnostic chest CT. All biopsy specimens were obtained at the area of maximal pleural thickening in the costal and parietal pleura. None of the biopsy samples was obtained from the mediastinal or diaphragmatic pleura. Lesion diameter perpendicular to the pleura ranged from 0.60 cm to 4.00 cm (median, 1.53 cm). The mean distance from the skin to the target was 3.40 ± 1.51 cm.

The mean total procedure time was 10.95 ± 4.58 minutes and the mean coaxial introducer indwelling time was 8.06 ± 4.00 minutes. Nineteen patients underwent biopsy in the supine position and 44 cases in the prone position. Cutting

Table 1. Procedural Records of 63 CBCT Virtual Navigation-Guided Pleural Biopsies in 59 Patients

Biopsy Records	Value (%)
Lesion size (perpendicular to pleura, cm)	1.53 ± 0.76
Lesion location (all costal pleura)	
Right	40/63 (63)
Left	23/63 (37)
Associated ipsilateral pleural effusion	24/63 (38) (15 loculated, 24)
Patient position	
Supine	19/63 (30)
Prone	44/63 (70)
Core needle biopsy	63/63 (100)
Skin to target distance (cm)	3.40 ± 1.51
Coaxial needle indwelling time (min)	8.06 ± 4.00
Total procedure time (min)	10.95 ± 4.58
Number of biopsies obtained	3.08 ± 1.34
Number of CBCT data acquisitions	3.11 ± 0.54

Data are mean ± standard deviation. CBCT = cone-beam CT

needle biopsy (18-gauge in 29 biopsies and 20-gauge in 34 biopsies) was performed in all cases. Tissue sampling was successful in all cases suggesting a technical success rate of 100%.

Among 62 cases with available dose data, 56 were analyzed using the Allura Xper FD20 system (Philips Healthcare), 3 cases with the AXIOM Artis system (Siemens Healthineers) and 3 cases with the Artis zee system (Siemens Healthineers). Mean DAP during the procedure was 12013.61 ± 7969.59 mGy·cm^2.

Pathologic Results, Diagnostic Accuracy and Complications

The total of 63 cases included 48 malignant (76.2%), 10 benign (15.9%), and 5 indeterminate (7.9%) lesions. The 48 malignant cases comprised 39 metastases (18 due to non-small cell lung cancer, 6 associated with small cell carcinoma, 1 from thymoma type B3 and 14 from extrathoracic malignancy), 3 cases of malignant mesothelioma, 2 cases of lymphoma involvement and 1 AML associated with the pleura (Fig. 1). Metastases originating in extrathoracic malignancies were as follows: 7 from breast cancer, 1 from high-grade myxofibrosarcoma, 1 from squamous carcinoma of the tongue, 2 from buccal cancer, 2 from HCC, and 1 from thyroid cancer with a pathology of poorly differentiated carcinoma consistent with metastatic carcinoma showing thymus-like differentiation. The 48 malignant lesions included 3 false-negative cases diagnosed with initial CBCT virtual navigation-guided biopsy, which was finally confirmed as metastasis originating in lung cancer (2 from non-small cell lung cancer [NSCLC] and 1 from SCLC) through repeat pleural biopsy.

Table 2. Comparison of Final Diagnosis with Results from CBCT-Guided Biopsy

CBCT-Guided Biopsy	Final Diagnosis of Malignancy	Final Diagnosis of Benign Disease
Positive for malignancy	45	0
Negative for malignancy	3	10

Five patients whose biopsy result was consistent with benign pathology with inadequate follow-up period (less than 2 years) were excluded from diagnostic performance calculation.

Of the 10 benign lesions, 3 demonstrated definitive benign pathology including tuberculosis (n = 1) (Fig. 2), leiomyoma (n = 1) and neurogenic tumor (n = 1). Three cases were finally confirmed surgically as fibromatosis (n = 2) and chronic inflammation with fibrosis (n = 1). One case of a pathological result of pleural tissue without tumor disappeared on follow-up CT and two cases with fibrous tissue and without tumor showed no change in interval on 2-year follow-up. One case of chronic active inflammation with granulomatous tissue formation decreased after treatment with anti-tuberculosis medication and was clinically diagnosed as tuberculosis of the pleura.

Five cases confirmed as pathologically benign according to biopsy were not followed up for 2 years and were recorded as indeterminate. These cases were excluded from the evaluation of diagnostic accuracy. Sensitivity, specificity, and accuracy of CBCT virtual navigation-guided pleural lesion biopsies were 93.8% (45/48), 100% (10/10), and 94.8% (55/58), respectively (Table 2).

There were three cases manifesting minimal post-procedural pneumothorax on chest radiograph obtained 3 hours later. However, there were no procedure-related immediate or subacute complications such as pneumothorax, hemoptysis, hemothorax or pleural effusion requiring intervention. Although the follow-up time to evaluate needle tract metastasis was too short in recent cases (median, 19 months; range, 6–78 months), there was no evidence of tract seeding on follow-up chest CT scans available.

DISCUSSION

Transthoracic needle biopsy is performed under fluoroscopy, CT, and ultrasonography guidance. The choice of imaging modality depends on the lesion characteristics

Korean Journal of Radiology
KJR

as well as radiologist's preference or accessibility to imaging systems (23). Several studies used ultrasound- or CT-guided cutting needle biopsy for suspicious malignant pleural lesions to date (Table 3) (9-14). To the best of our knowledge, however, this is the first study to evaluate the diagnostic accuracy of CBCT virtual navigation-guided percutaneous pleural biopsy, which revealed high accuracy (94.8%) for suspicious malignant pleural lesions. The results of our study are superior to the overall diagnostic sensitivity of previous studies investigating image-guided cutting needle pleural biopsy (9-14), with a sensitivity of 93.8% and specificity of 100%.

The CBCT virtual navigation system is known to increase the diagnostic accuracy via 3D visualization of target lesions, great flexibility in terms of the entry site and needle trajectory selection, and real-time guidance assisted with a "bull's eye" view. Pleural lesions are often narrow in width and are hard to target in the narrow needle insertion window. The aforementioned advantages of the CBCT virtual navigation system facilitate biopsy of pleural lesion. In particular, pleural lesions are not affected by respiration unlike pulmonary lesions, and thus, CBCT-guided biopsy is considered very appropriate for pleural biopsies. It also provides increased spatial room for operators for more precise targeting and planning even for small pleural lesions. Indeed, CBCT guidance has been used to address several limitations of CT-guided biopsy. These include the inability to provide real-time imaging guidance, the small gantry bore size leading to operator discomfort, limitations in imaging plane orientation due to the limited degree of gantry tilt resulting in difficulties with the selection of the optimal route to the target lesion (16, 24, 25). Although CT fluoroscopy system allows real-time imaging guidance, it is associated not only with the other challenges of CT-guided biopsy described above but also radiation exposure to the operator (26). Indeed, recent survey among the members of Korean Society of Thoracic Radiology reported that the majority of radiologists avoid using CT fluoroscopy (27).

In our study, no complications such as pneumothorax, hemothorax, hemoptysis, or air embolism requiring further intervention occurred. We believe that the use of the CBCT virtual navigation system partly contributed to safer biopsy in our patients. One of its biggest merits is the use of the "bull's eye view," which facilitated insertion of the coaxial needle system along the trajectory not only in the tangential but also oblique or angled fashion to the chest wall by aligning the detector, the skin entry site and the target. We also avoided the subcostal neurovascular bundle by freely selecting the path of needle insertion. Pleural lesions with a relatively thinner diameter were accurately sampled without any complications by performing biopsies along the pleural surface rather than tangentially. We also used the co-axial technique to reduce the number of needle insertions into the chest wall and minimize the risk of vessel injuries or visceral pleural penetration. In addition, the total procedure time was 10.95 ± 4.58 minutes. The

Table 3. Recent Studies on Percutaneous Image-Guided Cutting Needle Biopsy of Pleura

Authors	Year Published	Study Design	Biopsy Targets	Image Guidance	Sensitivity (%)	Specificity (%)	Complication Rates (%)
Scott et al. (9)	1995	Retrospective	Diffuse pleural thickening	CT	83	100	Hemoptysis: 1/45 (0.02) Air embolism: 1/45 (0.02)
Maskell et al. (10)	2003	Prospective	Pleural thickening with effusion	CT	87	100	None: 0/23 (0)
Adams et al. (11)	2001	Retrospective	Pleural thickening (pleural effusion negative: 7/21)	CT: 15/21 US: 6/21	86	100	Hemoptysis: 1/21 (0.05) Chest wall hematoma: 1/21 (0.05)
Adams and Gleeson (12)	2001	Retrospective	Pleural thickening with effusion (focal: 5/33, diffuse: 28/33)	CT: 24/33 US: 9/33	88	100	Chest wall hematoma: 1/33 (0.03)
Benamore et al. (13)	2006	Retrospective	Pleural thickening with or without effusion	CT: 80/85 US: 5/85	76	100	Pneumothorax: 4/85 (0.05)
Cao et al. (14)	2015	Retrospective	Pleural thickening (pleural effusion negative: 69/92)	CT	90.9	100	Pneumothorax: 6/92 (0.07) Pulmonary hemorrhage: 8/92 (0.09) Hemothorax: 1/92 (0.01)

US = ultrasonography

time spent for planning and calculation with the navigation software ranged between 1 minute and 2 minutes per case. Although no previous studies reported the procedural time of pleural lesion biopsy, we speculate that the total procedure time may have decreased due to the visualization of an imaginary prospective route and the operator's confidence even after the additional time to manipulate the virtual navigation software.

In terms of radiation exposure, the mean DAP in our study was 12013.61 mGvm^2. As the mean DAP in CBCT-guided lung nodule biopsy was 32880.0 (28), the radiation dose of CBCT-guided biopsy for pleural lesion may not be a substantial limitation. However, further efforts should be made to reduce the radiation dose by using a small field of view or by adjusting the collimation. One of the advantages of the CBCT-guided biopsy is that direct radiation dose to operator is significantly less compared with CT-fluoroscopy-guided biopsy.

There study limitations are as follows. First, our study included a relatively small number of patients. However, fewer pleural biopsies are conducted in routine practice compared with biopsies of lung nodules or mediastinal masses. Second, we did not examine the superiority of CBCT-guided biopsy in determining the diagnostic accuracy and complication rate compared with other methods of pleural lesion biopsy. Although prospective, randomized controlled trials may address this limitation, the CBCT virtual navigation-guided pleural lesion biopsy is still recommended with confidence considering the results of our experience.

In conclusion, CBCT virtual navigation-guided pleural biopsy is a highly accurate and safe diagnostic technique for suspicious pleural metastasis with reasonable radiation exposure and procedure time.

REFERENCES

1. Hussein-Jelen T, Bankier AA, Eisenberg RL. Solid pleural lesions. *AJR Am J Roentgenol* 2012;198:W512-W520
2. Evans AL, Gleeson FV. Radiology in pleural disease: state of the art. *Respirology* 2004;9:300-312
3. UyBico SJ, Wu CC, Suh RD, Le NH, Brown K, Krishnam MS. Lung cancer staging essentials: the new TNM staging system and potential imaging pitfalls. *Radiographics* 2010;30:1163-1181
4. Leung AN, Müller NL, Miller RR. CT in differential diagnosis of diffuse pleural disease. *AJR Am J Roentgenol* 1990;154:487-492
5. Cagle PT, Allen TC. Pathology of the pleura: what the pulmonologists need to know. *Respirology* 2011;16:430-438
6. Renshaw AA, Dean BR, Antman KH, Sugarbaker DJ, Cibas ES. The role of cytologic evaluation of pleural fluid in the diagnosis of malignant mesothelioma. *Chest* 1997;111:106-109
7. Hooper C, Lee YC, Maskell N; BTS Pleural Guideline Group. Investigation of a unilateral pleural effusion in adults: British Thoracic Society Pleural Disease Guideline 2010. *Thorax* 2010;65 Suppl 2:ii4-ii17
8. Lee P, Hsu A, Lo C, Colt HG. Prospective evaluation of flex-rigid pleuroscopy for indeterminate pleural effusion: accuracy, safety and outcome. *Respirology* 2007;12:881-886
9. Scott EM, Marshall TJ, Flower CD, Stewart S. Diffuse pleural thickening: percutaneous CT-guided cutting needle biopsy. *Radiology* 1995;194:867-870
10. Maskell NA, Gleeson FV, Davies RJ. Standard pleural biopsy versus CT-guided cutting-needle biopsy for diagnosis of malignant disease in pleural effusions: a randomised controlled trial. *Lancet* 2003;361:1326-1330
11. Adams RF, Gray W, Davies RJ, Gleeson FV. Percutaneous image-guided cutting needle biopsy of the pleura in the diagnosis of malignant mesothelioma. *Chest* 2001;120:1798-1802
12. Adams RF, Gleeson FV. Percutaneous image-guided cutting-needle biopsy of the pleura in the presence of a suspected malignant effusion. *Radiology* 2001;219:510-514
13. Benamore RE, Scott K, Richards CJ, Entwisle JJ. Image-guided pleural biopsy: diagnostic yield and complications. *Clin Radiol* 2006;61:700-705
14. Cao YY, Fan N, Xing F, Xu LY, Qu YJ, Liao MY. Computed tomography-guided cutting needle pleural biopsy: accuracy and complications. *Exp Ther Med* 2015;9:262-266
15. Jiao de C, Li TF, Han XW, Wu G, Ma J, Fu MT, et al. Clinical applications of the C-arm cone-beam CT-based 3D needle guidance system in performing percutaneous transthoracic needle biopsy of pulmonary lesions. *Diagn Interv Radiol* 2014;20:470-474
16. Choi JW, Park CM, Goo JM, Park YK, Sung W, Lee HJ, et al. C-arm cone-beam CT-guided percutaneous transthoracic needle biopsy of small (≤ 20 mm) lung nodules: diagnostic accuracy and complications in 161 patients. *AJR Am J Roentgenol* 2012;199:W322-W330
17. Choo JY, Park CM, Lee NK, Lee SM, Lee HJ, Goo JM. Percutaneous transthoracic needle biopsy of small (≤ 1 cm) lung nodules under C-arm cone-beam CT virtual navigation guidance. *Eur Radiol* 2013;23:712-719
18. Kim JI, Park CM, Lee SM, Goo JM. Rapid needle-out patient-rollover approach after cone beam CT-guided lung biopsy: effect on pneumothorax rate in 1,191 consecutive patients. *Eur Radiol* 2015;25:1845-1853
19. Lim WH, Park CM, Yoon SH, Lim HJ, Hwang EJ, Lee JH, et al. Time-dependent analysis of incidence, risk factors and clinical significance of pneumothorax after percutaneous lung biopsy. *Eur Radiol* 2018;28:1328-1337
20. Hwang EJ, Park CM, Yoon SH, Lim HJ, Goo JM. Risk factors for haemoptysis after percutaneous transthoracic needle biopsies

in 4,172 cases: focusing on the effects of enlarged main pulmonary artery diameter. *Eur Radiol* 2018;28:1410-1419
21. Kim H, Park CM, Lee SM, Goo JM. C-arm cone-beam CT virtual navigation-guided percutaneous mediastinal mass biopsy: diagnostic accuracy and complications. *Eur Radiol* 2015;25:3508-3517
22. Downer NJ, Ali NJ, Au-Yong IT. Investigating pleural thickening. *BMJ* 2013;346:e8376
23. Cheung JY, Kim Y, Shim SS, Lim SM. Combined fluoroscopy- and CT-guided transthoracic needle biopsy using a C-arm cone-beam CT system: comparison with fluoroscopy-guided biopsy. *Korean J Radiol* 2011;12:89-96
24. Carlson SK, Felmlee JP, Bender CE, Ehman RL, Classic KL, Hoskin TL, et al. CT fluoroscopy-guided biopsy of the lung or upper abdomen with a breath-hold monitoring and feedback system: a prospective randomized controlled clinical trial. *Radiology* 2005;237:701-708
25. Yankelevitz DF, Vazquez M, Henschke CI. Special techniques in transthoracic needle biopsy of pulmonary nodules. *Radiol Clin North Am* 2000;38:267-279
26. Nawfel RD, Judy PF, Silverman SG, Hooton S, Tuncali K, Adams DF. Patient and personnel exposure during CT fluoroscopy-guided interventional procedures. *Radiology* 2000;216:180-184
27. Jo Y, Han DH, Beck KS, Park JS, Kim TJ. Practice pattern of transthoracic needle biopsy: 2016 survey in the members of Korean society of thoracic radiology. *Korean J Radiol* 2017;18:1005-1011
28. Lee SM, Park CM, Lee KH, Bahn YE, Kim JI, Goo JM. C-arm cone-beam CT-guided percutaneous transthoracic needle biopsy of lung nodules: clinical experience in 1108 patients. *Radiology* 2014;271:291-300